

Emission of correlated electron pairs following single-photon absorption by solids and surfaces

Jamal Berakdar

Max-Planck Institute for Microstructure Physics, Weinberg 2, 06120 Halle, Saale, Germany

(Received 23 March 1998)

The simultaneous emission of two electrons from condensed matter following the absorption of a linearly polarized photon is studied in the first order-perturbation theory for the radiation field, and within the dipole approximation. The double emission from localized and delocalized electronic states is considered. It is shown that spectra of the emitted pairs obey propensity rules expressed by the scalar product of the center-of-mass vector momentum of the pair and the photon's polarization vector. Furthermore, it is shown that diffraction of the pair from the lattice occurs when the pair's center-of-mass wave vector changes by a lattice reciprocal vector during the photoemission. For semi-infinite solids with delocalized valence electrons, an initial state is constructed from single-particle orbitals. Following the absorption of the photon the valence-band electron pair propagates into the vacuum within the screened electron-electron Coulomb potential. Numerical results for a clean Cu crystal are analyzed for photon polarization parallel and perpendicular to the surface.

[S0163-1829(98)09439-9]

I. INTRODUCTION

Over the last few decades angular- and spin-resolved ultraviolet single-photoemission spectroscopy (ARUPS) emerged as a powerful and widely used method to investigate the electronic structure of crystalline materials.^{1,2} This development has been driven by the growing demand for a detailed knowledge of technologically relevant physical properties of solids and their surfaces, e.g., catalytic reactions are mainly controlled by the electronic and geometric structure of surfaces.

Theoretical treatments of ARUPS are of special importance as they provide the linkage between the photocurrent measurements and the corresponding band structure.¹⁻³ A standard successful scheme for band-structure calculations relies on density-functional theory (DFT),⁴ in which the electronic many-body problem is solved in a one-electron picture. *Spatially uncoupled single-particle* states are then determined self-consistently using an approximate expression for the exchange and correlation term.⁵ Many aspects of the emission process are described within this single-particle picture, as a transition from an occupied one-electron orbital to a state describing the propagation of the photoelectron. The complicated many-body nature of the solid is then collectively subsumed in the screening and decay of the photoelectron, and the hole left behind. These screened, decaying quasiparticles can still be described by a single-particle wave equation. Experimental evidence for many-body effects shows up as subsidiary features in the photoelectron spectra.

In contrast, and as explicitly shown in the present work, a simultaneous two-orbital excitation by one photon is prohibited if *spatial* coupling between these orbitals is absent. Therefore, dealing with this process, the description of the electron-electron interaction must go beyond regarding it as a collective, spatially independent perturbation of the single-particle orbitals. Thus it seems worthwhile to employ double photoemission (DPE) as an investigative tool for strongly correlated systems, such as Mott insulators, ferromagnetic materials with *d* and *f* levels, and high-temperature superconductors. In fact, as shown in this paper, to some extent DPE can be regarded as single photoemission of a "quasiparticle"

formed by the electron pair. In addition to the known features of ARUPS, the spectra of this photoemitted "quasiparticle" reveal a dependence on the pair's internal degree of freedom that characterizes the mutual interaction of the two emitted electrons. Therefore, DPE experiments are expected to provide a direct insight into the influence of electronic correlation on initial and final many-body states.

In atomic and molecular physics, the explicit dependence of DPE on the interelectronic correlation is well established.⁶ The first experiment of this kind on a He($1S^e$) target was performed in 1993,⁷ followed by a series of experiments on different targets at a variety of scattering geometries.⁸⁻¹² The theoretical treatments stimulated by these experiments revealed the strong dependence of this reaction on the detail of mutual electronic coupling,^{8,13,15,14,16} as well as on properties of the radiation field.^{17,18} Very recently DPE from He($1S^e$) with circularly polarized photons has been observed.^{19,20}

DPE from Ni(001) and Cu(001) has just been reported.²¹ Thus it is appropriate to consider DPE theoretically from solids and surfaces. Starting from the first-order perturbation theory and the dipole approximation for the photon field, a formal expression for the cross section of DPE is derived (transition rate normalized to the incoming photon-flux density). Subsequently, DPE from localized bulk states is studied and propensity rules are inferred. DPE from delocalized valence electrons is then investigated, and the selection rules in this case are discussed. Numerical examples for DPE from a clean Cu crystal are presented for *p* and *s* polarizations. Atomic units (a.u.) are used throughout.

II. THEORETICAL FRAMEWORK

For the derivation of the transition amplitude for simultaneous electron ejection, it is instructive to specify the properties of the radiation field. In what follows we assume a large photon density, so that the electromagnetic field can be treated classically (an upper limit for the photon density of concern here is given below). We operate in the Coulomb gauge, i.e., $\nabla \cdot \mathbf{A} = 0$, so that, in vacuum, we can set $\Phi = 0$,

where \mathbf{A} and Φ are the field vector and scalar potentials, respectively. It should be noted from the outset, however, that near a surface \mathbf{A} may change rapidly which invalidates the assumption $\nabla \cdot \mathbf{A} = 0$ unless the dielectric constant ϵ is unity.^{22,23} To avoid this case the photon energies have to be well above the plasmon energies.²⁴ For \mathbf{A} we assume a monochromatic, plane-wave solution with a wave vector \mathbf{k} , which is related to the photon frequency ω via $k = \alpha\omega$, where α is the fine-structure constant. The energy density ρ of the (classical) radiation field averaged over the period $T = 2\pi/\omega$ is given by $\rho = \omega^2 A^2 / (2\pi)$. Thus the energy-flux density, i.e., the intensity I , is given by $I = \rho/\alpha$. For a low-intensity field we can set $A^2 \approx 0$ (for $A \approx 0.01$ and a photon energy of 50 eV we arrive at a maximum intensity $I \approx 5 \times 10^{17}$ W/m²). We assume the unperturbed system to be described by the Hamiltonian H , and to be in the stationary state $|i\rangle$ with energy ϵ_i , i.e.,

$$(H - \epsilon_i)|i\rangle = 0. \quad (1)$$

Under the time-dependent action of the photon field the system performs, within a time lap τ , a transition into vacuum states $|f\rangle$ which lay within the interval β and $\beta + d\beta$, where β stands for collective quantum numbers that specify the final channel.

In a time-dependent first-order perturbation treatment (only photoabsorption is considered here), a transition probability dw_{if} can be derived.²⁵ Thus we can define a transition rate $dP_{if} = dw_{if}/\tau$ that can be deduced to

$$dP_{if} = (2\pi)^2 \frac{I\alpha}{\omega^2} \sum_{\alpha_i} |\langle f | \tilde{W}_0 | i \rangle|^2 \delta(E_f - E_i) d\beta, \quad (2)$$

where E_f is the total energy in the final channel and $E_i = \omega + \epsilon_i$. Equation (2) sums over the unresolved quantum numbers α_i in the initial state. The perturbation \tilde{W}_0 in Eq. (2) amounts to

$$\tilde{W}_0 = A \sum_{j=1}^N \exp[i(\mathbf{k} \cdot \mathbf{r}_j)] \hat{\mathbf{e}} \cdot \mathbf{p}_j, \quad (3)$$

where \mathbf{p}_j are the one-particle momentum operators and $\hat{\mathbf{e}}$ is the polarization vector.

As the differential cross section $d\sigma/d\beta$ we define the transition rate normalized to the incoming flux density I/ω , i.e.,

$$d\sigma = \omega dP_{if}/I. \quad (4)$$

In this work we consider moderate photon energies (< 500 eV), and we can thus operate within the dipole approximation. In this case Eq. (4) reduces to

$$d\sigma = 4\pi^2 \frac{\alpha}{\omega} \sum_{\alpha_i} |M_{fi}|^2 \delta(E_i - E_f) d\beta, \quad (5)$$

where the dipole-matrix element is given by

$$M_{fi} = \sum_j^N \langle f | \hat{\mathbf{e}} \cdot \mathbf{p}_j | i \rangle. \quad (6)$$

By making use of the canonical commutation relations $-i[\mathbf{r}_j, H] = \mathbf{p}_j$, and assuming that $|i\rangle$ and $|f\rangle$ are eigenfunctions of the *same* Hamiltonian H , the *velocity form* Eq. (9) can be converted into the *length form*

$$d\sigma = 4\pi^2 \alpha \omega \sum_{\alpha_i} \left| \sum_j^N \langle f | \mathbf{r}_j | i \rangle \right|^2 \delta(E_f - E_i) d\beta. \quad (7)$$

In practice, $|i\rangle$ and $|f\rangle$ are derived using different approximate procedures for H , and thus the velocity and length forms yield, in general, different predictions. Conversely, equivalent cross sections, calculated within the length and velocity forms, mean merely that the same approximations have been made in the initial and final channel, but they say, however nothing about the quality of these approximations. Nevertheless, it is desirable to choose $|i\rangle$ and $|f\rangle$ as eigenstates of the same (approximate) Hamiltonian to preclude spurious transitions in the absence of the perturbation \tilde{W}_0 .

Regardless of the form in which the dipole operator is presented, its mathematical structure is always a sum of single-particle operators. This has the following important consequence: If we assume $|i\rangle$ and $|f\rangle$ to be written in terms of orthonormal single-particle orbitals $\phi_j(\mathbf{r}_j)$, in the simplest case as

$$\begin{aligned} \langle \mathbf{r}_1 \cdots \mathbf{r}_N | i \rangle &= \prod_j^N \phi_{i,j}(\mathbf{r}_j), \\ \langle \mathbf{r}_1 \cdots \mathbf{r}_N | f \rangle &= \prod_j^N \phi_{f,j}(\mathbf{r}_j), \end{aligned} \quad (8)$$

then the matrix element (6) is finite for single-orbital excitation, only, e.g., single photoemission. In other words, DPE is prohibited in a single-particle picture. This is readily concluded in the simplest case of two orbital excitation ϕ_l, ϕ_k , which is the minimal requirement for DPE:

$$\begin{aligned} M_{fi} &= \langle \phi_{f,k} \phi_{f,l} | \hat{\mathbf{e}} \cdot \mathbf{p}_l | \phi_{i,k} \phi_{i,l} \rangle + \langle \phi_{f,k} \phi_{f,l} | \hat{\mathbf{e}} \cdot \mathbf{p}_k | \phi_{i,k} \phi_{i,l} \rangle \\ &= \langle \phi_{f,k} | \phi_{i,k} \rangle \langle \phi_{f,l} | \hat{\mathbf{e}} \cdot \mathbf{p}_l | \phi_{i,l} \rangle \\ &\quad + \langle \phi_{f,l} | \phi_{i,l} \rangle \langle \phi_{f,k} | \hat{\mathbf{e}} \cdot \mathbf{p}_k | \phi_{i,k} \rangle \\ &= \delta_{i,f} (\langle \phi_{f,k} | \hat{\mathbf{e}} \cdot \mathbf{p}_k | \phi_{i,k} \rangle + \langle \phi_{f,l} | \hat{\mathbf{e}} \cdot \mathbf{p}_l | \phi_{i,l} \rangle), \end{aligned} \quad (9)$$

where $\phi_{i,k}, \phi_{i,l}$ ($\phi_{f,k}, \phi_{f,l}$) are the participating single particle orbitals in the initial (final) channel. From Eq. (9) it follows that DPE is a direct signature of coupling between single-particle orbitals, at least those of the electrons simultaneously detected in the final state, i.e., the two photoelectrons must be correlated in initial and/or final state. This conclusion is also valid for an antisymmetrized product of spatially independent single-particle orbitals. It should be stressed that Eq. (9) and the single-particle nature of the perturbation [Eq. (3)] do not mean that the photon can only be absorbed by one electron, and the other electron is emitted by means of coupling or inelastic scattering with the former one. To see this, let us assume the holes created by the process to be long lived on the scale of the characteristic interaction time τ and neglect any phonon excitation. In this case a frozen-core approximation is appropriate. In addition, if the

photoelectrons are represented by the correlated initial (final) state $\psi_i(\mathbf{r}_l, \mathbf{r}_k)$ [$\psi_f(\mathbf{r}_l, \mathbf{r}_k)$] we can always canonically transform to the coordinate system $\mathbf{r}^+ = (\mathbf{r}_l + \mathbf{r}_k)/2$, $\mathbf{r}^- = \mathbf{r}_l - \mathbf{r}_k$. In this case the photoabsorption matrix element (6) takes on the (length) form $M_{fi} = \langle \psi_f(\mathbf{r}^+, \mathbf{r}^-) | \hat{\mathbf{e}} \cdot \mathbf{r}^+ | \psi_i(\mathbf{r}^+, \mathbf{r}^-) \rangle / 2$ which means that the photon is absorbed by the center-of-mass coordinate \mathbf{r}^+ of the two-electron system. This *simultaneous* photoabsorption is fundamentally distinct from the process of single photoemission accompanied by secondary vacuum-electron creation.

III. DOUBLE PHOTOEMISSION FROM LOCALIZED ELECTRONIC STATES

In the rest of this work we assume a frozen-core approximation, i.e., only the degrees of freedom of the two emitted electrons are affected by the photoabsorption process. To obtain an insight into the structure of the matrix element M_{fi} , we consider first the DPE of localized electrons, e.g., core electronic states or valence-band electrons of insulators. The initial state can then be described by a tight-binding two-electron wave function, whereas the vacuum motion of the electrons is assumed to be free and characterized by the momenta \mathbf{k}_a and \mathbf{k}_b , as measured in a coincidence experiment (uncorrelated final-state Bloch waves lead basically to the same conclusion). Equation (6) can be written in the form

$$M_{fi}(\mathbf{k}_a, \mathbf{k}_b) = C \sum_l \int \int d^3\mathbf{r}_a d^3\mathbf{r}_b \times \exp(-i\mathbf{k}_a \cdot \mathbf{r}_a - i\mathbf{k}_b \cdot \mathbf{r}_b) \exp[i(\mathbf{k}'_a + \mathbf{k}'_b) \cdot \mathbf{R}_l] \times [\hat{\mathbf{e}} \cdot (\mathbf{p}_a + \mathbf{p}_b)] \phi_i(\mathbf{r}_a - \mathbf{R}_l, \mathbf{r}_b - \mathbf{R}_l). \quad (10)$$

where \mathbf{R}_l designates the core sites, and ϕ_i describes the localized two-electron initial state with Bloch wave vectors \mathbf{k}'_a and \mathbf{k}'_b . The constant C derives from the normalization of the initial- and final-state wave functions. After some elementary manipulation the magnitude of $M_{fi}(\mathbf{k}_a, \mathbf{k}_b)$ is reduced to

$$|M_{fi}|^2 = |C|^2 \delta_{(\mathbf{q}_i - \mathbf{q}_f, \mathbf{G})}^{(3)} |M_{fi}^{atom}|^2, \quad (11)$$

where $\mathbf{q}_i = \mathbf{k}'_a + \mathbf{k}'_b$, $\mathbf{q}_f = \mathbf{k}_a + \mathbf{k}_b$ are the wave vectors of the pair's center of mass in the initial and final states, respectively, and \mathbf{G} is a bulk reciprocal-lattice vector. The atomic matrix element M_{fi}^{atom} is given by

$$M_{fi}^{atom}(\mathbf{k}_a, \mathbf{k}_b) = \int \int d^3\mathbf{r} d^3\mathbf{r}' \exp(-i\mathbf{k}_a \cdot \mathbf{r} - i\mathbf{k}_b \cdot \mathbf{r}') \times [\hat{\mathbf{e}} \cdot (\mathbf{p}_a + \mathbf{p}_b)] \phi_i(\mathbf{r}, \mathbf{r}'). \quad (12)$$

In momentum-space representation

$$M_{fi}^{atom}(\mathbf{k}_a, \mathbf{k}_b) = \int \int d^3\mathbf{p} d^3\mathbf{p}' \langle \mathbf{k}_a, \mathbf{k}_b | \hat{\mathbf{e}} \cdot (\mathbf{p}_a + \mathbf{p}_b) | \mathbf{p}, \mathbf{p}' \rangle \times \langle \mathbf{p}, \mathbf{p}' | \phi_i \rangle = \hat{\mathbf{e}} \cdot (\mathbf{k}_a + \mathbf{k}_b) \tilde{\phi}_i(\mathbf{k}_a, \mathbf{k}_b). \quad (13)$$

In Eq. (13) $|\mathbf{p}, \mathbf{p}'\rangle$ denotes a complete set of plane waves, and $\tilde{\phi}_i(\mathbf{k}_a, \mathbf{k}_b)$ is the double Fourier transform of the initial state. Note that Eqs. (12) and (13) do not factorize in single-particle contributions due to the correlated state $\phi_i(\mathbf{r}, \mathbf{r}')$. From Eqs. (11)–(13), three important conclusions are drawn.

(a) According to the von Laue-like conditions in Eq. (11), diffraction of the pair occurs when the center-of-mass momentum of the pair changes by a reciprocal bulk vector due to the emission process. This (and the selection rules stated below) is equivalent to assuming the pair as a quasiparticle with momentum $\mathbf{k}_a + \mathbf{k}_b$ (the pair's center-of-mass momentum) and performing single photoemission of this quasiparticle.

(b) The selection rules for M_{fi}^{atom} can be summarized in the equation $\hat{\mathbf{e}} \cdot (\mathbf{k}_a + \mathbf{k}_b) = 0$, i.e., double photoemission is forbidden if the momentum of the two-electron center of mass is perpendicular to the polarization vector $\hat{\mathbf{e}}$ or if $\mathbf{k}_a = -\mathbf{k}_b$. In addition the structure of $\tilde{\phi}_i(\mathbf{k}_a, \mathbf{k}_b)$, which is very much dependent on the symmetry of the investigated core level, imposes additional restrictions on the DPE spectra. These conclusions remain valid if we allow for mutual repulsion of the outgoing electrons, but disregard the final-channel coupling to the cores. This can be deduced in a similar manner as in Eq. (22). In cases where the motion of the vacuum electrons is influenced by the core potentials, atomic selection rules for the double photoionization applies.^{13,16,17}

(c) If the magnetic sublevels of the two-electron orbital ϕ_i are statistically populated (which is usually the case), then $|M_{fi}|^2$, and hence the cross section, shows in general a *circular dichroism* with respect to inversion of the helicity of the incoming radiation. This is readily deduced from the analysis performed in Refs. 17 and 18. Note that, in the absence of a preferential orientation of the initial state and a spin analysis of the photoelectrons, as assumed in this work, the aforementioned dichroism vanishes identically for single photoemission.¹⁸

IV. DOUBLE PHOTOEMISSION OF DELOCALIZED ELECTRONIC STATES

In this section we consider double photoemission from *s-p* bonded (simple) metal surfaces like Na and Al. In this case the cores scatter the conduction-band electrons only weakly. The momentum distribution of the conduction-band electrons can then, to a good approximation, be simulated by jellium states. In the jellium model the ionic cores are smeared to a uniform constant positive ‘‘background charge.’’ The electrons are bound to the metal half-space ($z < 0$) by the step-potential barrier V_0 (at $z = 0$)

$$V_0 = \epsilon_F + W, \quad (14)$$

where ϵ_F is the Fermi energy and W is the work function. Within the metal volume V the conduction-band electrons are treated as free particles. The density of states ρ_{DOS} is given by that of the free-electron gas (apart from a factor 2 due to electronic spin states) $\rho_{DOS} = V/(4\pi^3)$. As the binding potential V_0 is steplike, the single-particle jellium wave

function $\phi_{\epsilon_j(\mathbf{k}'_j), \mathbf{k}'_j}(\mathbf{r}_j)$, with binding energy $\epsilon_j(\mathbf{k}'_j)$ and wave vector \mathbf{k}'_j , can be represented in terms of reflection and transmission coefficients:

$$\phi_{\epsilon_j(\mathbf{k}'_j), \mathbf{k}'_j}(\mathbf{r}_j) = \frac{1}{\sqrt{V}} \exp(i\mathbf{k}'_{j,\parallel} \cdot \mathbf{r}_{j,\parallel}) \times \begin{cases} e^{i\mathbf{k}'_{j,z} z_j + \text{Re}^{-i\mathbf{k}'_{j,z} z_j} & z < 0, \\ T e^{-\gamma z_j} & z > 0, \end{cases} \quad (15)$$

where $\mathbf{k}'_{j,z}$ and z_j are, respectively, the components of $\mathbf{k}'_j, \mathbf{r}_j$ with respect to the normal of the surface (pointing into the vacuum), and $\mathbf{k}'_{j,\parallel}, \mathbf{r}_{j,\parallel}$ are the corresponding components parallel to the surface. The reflection and transmission coefficients R and T are given by

$$R = \frac{\mathbf{k}'_{j,z} - i\gamma}{\mathbf{k}'_{j,z} + i\gamma}, \quad T = \frac{2\mathbf{k}'_{j,z}}{\mathbf{k}'_{j,z} + i\gamma} \quad (16)$$

and $\gamma = \sqrt{2V_0 - \mathbf{k}'_j{}^2}$.

As in the jellium model the electrons are considered to be quasifree, for the two-electron initial state $|i\rangle$ we employ a (singlet) symmetrized direct product of two jellium single-particle states, i.e.,

$$|\psi_{\epsilon_i; \mathbf{k}'_a, \mathbf{k}'_b}(\mathbf{r}_a, \mathbf{r}_b)\rangle \approx \frac{1}{\sqrt{2}} [|\phi_{\epsilon_a, \mathbf{k}'_a}(\mathbf{r}_a)\rangle \otimes |\phi_{\epsilon_b, \mathbf{k}'_b}(\mathbf{r}_b)\rangle + |\phi_{\epsilon_a, \mathbf{k}'_b}(\mathbf{r}_b)\rangle \otimes |\phi_{\epsilon_b, \mathbf{k}'_a}(\mathbf{r}_a)\rangle]. \quad (17)$$

The total binding energy ϵ_i of this state is $\epsilon_i = \epsilon_a(\mathbf{k}'_a) + \epsilon_b(\mathbf{k}'_b)$ with parabolic dispersion for the *single* particle states. State (17) is energetically favored with respect to its antisymmetric (triplet) counterpart.

As the initial state [Eq. (17)] does not contain any inter-electronic coupling, it is essential to incorporate the inter-electronic interaction in the final state. To this end we note that the asymptotic two-electron vacuum state $|\mathbf{k}_a, \mathbf{k}_b\rangle$, that is defined by the measured momenta \mathbf{k}_a and \mathbf{k}_b , where $E_f = E_a + E_b$ and $E_a = k_a^2/2$, $E_b = k_b^2/2$ are the electrons' energies, is an eigenstate of the two-electron kinetic-energy operator K , i.e.,

$$K|\mathbf{k}_a, \mathbf{k}_b\rangle = \frac{1}{2}(\mathbf{p}_a^2 + \mathbf{p}_b^2)|\mathbf{k}_a, \mathbf{k}_b\rangle = E_f|\mathbf{k}_a, \mathbf{k}_b\rangle. \quad (18)$$

The final state $|f\rangle$ is then obtained by the time-reversed evolution (back to the time of absorption) mediated by the Møller operator $\Omega^- = (1 + G^-V)$,²⁶ i.e.,

$$|f\rangle = [1 + G^-(H - K)]|\mathbf{k}_a, \mathbf{k}_b\rangle = (1 + G^-V)|\mathbf{k}_a, \mathbf{k}_b\rangle, \quad (19)$$

where G^- is the resolvent (Green operator) of total Hamiltonian H which satisfies the Dyson equation

$$G^- = G_0^- + G_0^- V G^-, \quad (20)$$

and G_0 is the Green operator of the noninteracting system (with outgoing wave boundary conditions). Contrasting the state vector (19) with that used in single photoemission,¹ it can be said that $|f\rangle$ is the time-reversed low-energy electron-diffraction (LEED) state of the coupled electron pair.²⁴

From Eqs. (19) and (20), it is evident that, after absorption of the photon, the two electrons interact with all degrees of freedom of the system, described by H (such as diffraction from the lattice, elastic, and inelastic collisions and collective excitations) before emerging with the asymptotic momenta \mathbf{k}_a and \mathbf{k}_b . These interactions are basically contained in the complex two-particle self-energy V that appears in Eqs. (20) and (19).^{3,27,28} The non-Hermitian character of V accounts for damping processes of the photoelectron flux and energetic shifts in the quasi-particle spectrum. Considering the difficulties encountered in adequately estimating the *single*-particle self energy,³ it is obvious that calculating the two-particle self-energy is a very delicate problem. Hence, we replace it in the rest of this work by the (real) potential. In addition, as the electron-electron interaction V_{ee} is inevitable for coherent DPE we regard this interaction as the ‘‘strong’’ potential with respect to the surface-photoelectron coupling, i.e., we employ the approximation $V \approx V_{ee}$. For V_{ee} we assume a screened Coulomb potential, with the screening constant derived from the Thomas-Fermi model.²⁹ Under these circumstances Eq. (19) reduces to

$$|f\rangle \approx (1 + G_{ee}^- V_{ee})|\mathbf{k}_a, \mathbf{k}_b\rangle, \quad (21)$$

with G_{ee}^- being the propagator within the potential V_{ee} . With Eqs. (21) and (17), we can now obtain an estimate of the transition probability M_{fi} , given by Eq. (6). Since V_{ee} and G_{ee} are dependent on interelectronic degrees of freedom only, properties of M_{fi} are most transparent in the representation $\mathbf{r}^+ \otimes \mathbf{r}^-$ that, as previously mentioned, can be canonically mapped onto $\mathbf{r}_a \otimes \mathbf{r}_b$ [$\mathbf{r}^+ = (\mathbf{r}_a + \mathbf{r}_b)/2, \mathbf{r}^- = \mathbf{r}_a - \mathbf{r}_b$]. Equation (6) reads

$$M_{fi}(\mathbf{k}^-, \mathbf{k}^+) = \int \int d^3\mathbf{q}^- d^3\mathbf{q}^+ \langle \mathbf{k}^-, \mathbf{k}^+ | (1 + V_{ee} G_{ee}^+) (\hat{\mathbf{e}} \cdot \mathbf{p}^+) | \mathbf{q}^-, \mathbf{q}^+ \rangle \langle \mathbf{q}^-, \mathbf{q}^+ | \psi \rangle = \hat{\mathbf{e}} \cdot \mathbf{k}^+ \left[\tilde{\psi}(\mathbf{k}^+, \mathbf{k}^-) + \int d^3\mathbf{q}^- \langle \mathbf{k}^- | V_{ee} G_{ee}^+ | \mathbf{q}^- \rangle \langle \mathbf{q}^-, \mathbf{k}^+ | \psi \rangle \right], \quad (22)$$

where $\mathbf{k}^- = (\mathbf{k}_a - \mathbf{k}_b)/2$, $\mathbf{k}^+ = \mathbf{k}_a + \mathbf{k}_b$, and $|\mathbf{q}^-, \mathbf{q}^+\rangle$ is a complete set in the space reciprocal to $\mathbf{r}^+ \otimes \mathbf{r}^-$.

According to Eq. (22) the propensity rules $\hat{\mathbf{e}} \cdot \mathbf{k}^+ = 0$, as discussed in Sec. III, apply. As it is clear from the derivation of Eq. (22) these rules do not depend on the structure of the initially bound state $|\psi\rangle$. They are rather an immediate consequence of the approximation made to arrive at Eq. (21).

V. CALCULATION OF THE DIPOLE-MATRIX ELEMENT

In spite of the simple analytical structure of the wave function (17), the evaluation of the transition amplitude (22) is mathematically involved and, till now, only possible within the approximation $G_{ee}^+ \approx G_0^+$, i.e., in LEED language, within the kinematical approximation.³⁰ The derivation of M_{fi} is presented in the Appendix. The final result can be written as

$$M_{fi}(\mathbf{k}_a, \mathbf{k}_b) = \langle \mathbf{k}_a, \mathbf{k}_b | (1 + V_{ee} G_0^+) [\hat{\mathbf{e}} \cdot (\mathbf{p}_a + \mathbf{p}_b)] | \psi_{\epsilon_i} \rangle = T_{\text{spe}} + T_{\text{dpe}}, \quad (23)$$

where

$$\begin{aligned} T_{\text{spe}} &= \langle \mathbf{k}_a, \mathbf{k}_b | \hat{\mathbf{e}} \cdot (\mathbf{p}_a + \mathbf{p}_b) | \psi_{\epsilon_i} \rangle \\ &= -(\hat{\mathbf{e}} \cdot \mathbf{k}_a + \hat{\mathbf{e}} \cdot \mathbf{k}_b) \delta^{(2)}(\mathbf{k}'_{a,\parallel} - \mathbf{k}_{a,\parallel}) \delta^{(2)}(\mathbf{k}'_{b,\parallel} - \mathbf{k}_{b,\parallel}) \frac{\pi \sqrt{2}}{V} [L_{\mathbf{k}'_a}(\mathbf{k}_a) L_{\mathbf{k}'_b}(\mathbf{k}_b) + L_{\mathbf{k}'_b}(\mathbf{k}_a) L_{\mathbf{k}'_a}(\mathbf{k}_b)] \end{aligned} \quad (24)$$

and

$$\begin{aligned} T_{\text{dpe}} &= \langle \mathbf{k}_a, \mathbf{k}_b | V_{ee} G_0^+ [\hat{\mathbf{e}} \cdot (\mathbf{p}_a + \mathbf{p}_b)] | \psi_{\epsilon_i} \rangle \\ &= \hat{\mathbf{e}} \cdot (\mathbf{k}_a + \mathbf{k}_b) \delta^{(2)}[(\mathbf{k}'_{a,\parallel} + \mathbf{k}'_{b,\parallel}) - (\mathbf{k}_{a,\parallel} + \mathbf{k}_{b,\parallel})] \frac{1}{\sqrt{8\pi V}} [I(\epsilon_a, \mathbf{k}'_a, \epsilon_b, \mathbf{k}'_b; \mathbf{k}_a, \mathbf{k}_b) + I(\epsilon_b, \mathbf{k}'_b, \epsilon_a, \mathbf{k}'_a; \mathbf{k}_a, \mathbf{k}_b)]. \end{aligned} \quad (25)$$

The functions $I(\epsilon_a, \mathbf{k}'_a, \epsilon_b, \mathbf{k}'_b; \mathbf{k}_a, \mathbf{k}_b)$ and $L_{\mathbf{k}'_j}(\mathbf{k}_j)$, $j = a, b$, are given by Eqs. (A9) and (A4), respectively. Equations (24) and (25) reflect the basic difference between single and simultaneous double photoemission: Term (24) contains no final-state correlation of the pairs. The DPE is then regarded as two independent single photoemission processes. Consequently, the surface components of the wave vectors of the *individual* electrons is conserved during the ejection, and for each absorption process the selection rules for the single photoemission apply. In contrast, as a result of including electronic correlation in Eq. (25) only the surface component of the pair's center-of-mass wave vector is invariant during the reaction. Under this constraint the surface components of the wave vectors of the individual electrons may well not be conserved (due to momentum exchange). As mentioned in the preceding sections, the amplitude [Eq. (24)] must vanish, for initial- and final-state electronic correlation are disregarded. In fact extensive numerical calculations have shown that $|T_{\text{spe}}|$ is negligible with respect to $|T_{\text{dpe}}|$ (typically six order of magnitudes smaller).

Double emission probabilities

In a recent double photoemission experiment²¹ on Cu(001) and Ni(001), the coincidence rate has been measured as function of \mathbf{k}_a , \mathbf{k}_b , and ω . The Bloch wave vectors of the initially bound electronic states were not specified [actually a Bloch wave vector of the electron pair is a more appropriate designation of these states (cf. Eq. (25)]. Thus, Eq. (5) yields

$$\begin{aligned} d\sigma &= 4\pi^2 \frac{\alpha}{\omega} \int \int d^3\mathbf{k}'_a d^3\mathbf{k}'_b \rho(\mathbf{k}'_a) \\ &\quad \times F(\mathbf{k}'_a, T) \rho(\mathbf{k}'_b) F(\mathbf{k}'_b, T) |M_{fi}|^2 \delta(E_i - E_f) \\ &\quad \times d^3\mathbf{k}_b d^3\mathbf{k}_a d^3\mathbf{k}_{\text{rec}}, \end{aligned} \quad (26)$$

where \mathbf{k}_{rec} is related to the recoil momentum of the crystal (free electrons cannot absorb the photon). The one-particle density of states at the temperature T is referred to as $\rho(\mathbf{k}'_j)$, $j = a, b$, and $F(\mathbf{k}'_j, T)$ is the Fermi distribution. The initial total energy E_i can be estimated assuming the conduction band of the pair as being formed of independent bands of the single electrons, i.e., $E_i = \omega - 2W - \epsilon_a(\mathbf{k}'_a) - \epsilon_b(\mathbf{k}'_b)$. (In contrast to atomic systems, this approximation is reasonable due to the collective screening of the electron-electron interaction). In Eq. (26) the dependence of σ on \mathbf{k}_{rec} is fixed by the conservation of linear momentum.

For the approximate initial state [Eq. (17)] which leads to the matrix element (23) and at $T = 0$, Eq. (26) simplifies to

$$\begin{aligned} d\sigma &= \frac{V^2 \alpha}{4\pi^4 \omega} \left[\int_{k'_a \leq k_F} \int_{k'_b \leq k_F} d^3\mathbf{k}'_a d^3\mathbf{k}'_b |M_{fi}|^2 \right. \\ &\quad \left. \times \delta(E_i - E_f) \right] d^3\mathbf{k}_b d^3\mathbf{k}_a, \end{aligned} \quad (27)$$

where k_F is the Fermi momentum for the single-particle band. The six-dimensional integral in Eq. (27) can be analytically reduced to three-dimensional ones that have been performed numerically.

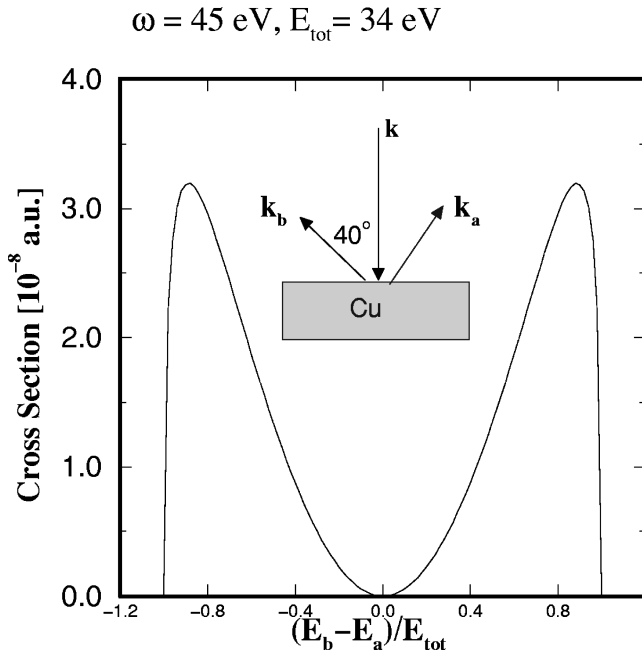


FIG. 1. The double-photoemission cross section [Eq. (27)] as function of the energy sharing of two electrons emitted from a clean Cu monocrystal upon the absorption of a linearly polarized photon. The photon's wave vector \mathbf{k} is normal to the surface, whereas the electron detectors are fixed at 40° to the left and right of \mathbf{k} (see the inset). The photon incident energy is $\omega = 45$ eV, and the total excess energy of the pair is chosen as $E_{\text{tot}} = E_a + E_b = 34$ eV.

Employing Eq. (27), we consider the energy sharing of the two-photoelectron pair emitted from Cu(001) for s -photon polarization (see the inset in Fig. 1). As the electron detectors have the same relative angles with respect to the wave vector of the photons (the inset in Fig. 1), the vector

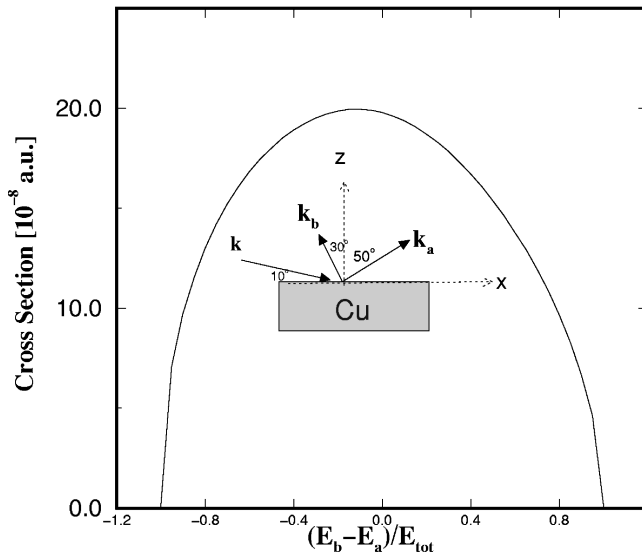


FIG. 2. Same energies as Fig. 1; however, as demonstrated by the inset, the photon beam is now in grazing incidence (10° with respect to the surface). One of the electron detectors (say detector a) is fixed right to the surface normal at an angle of 50° , whereas the other detector is positioned left the surface normal at an angle of 30° . The coordinate system and the geometry are sketched in the inset.

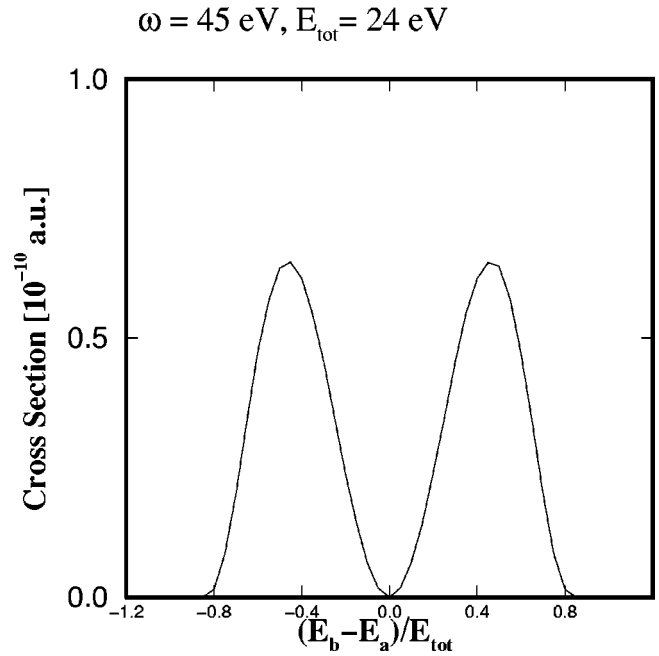


FIG. 3. Same geometry as in Fig. 1, with the same incident photon energy; however, the total excess energy of the pair is lowered to $E_{\text{tot}} = 24$ eV.

momentum of the pair $\mathbf{k}_a + \mathbf{k}_b$ is perpendicular to the surface, and hence to the polarization vector, for equal-energy electrons. Consequently, double photoemission is forbidden for $k_a = k_b$, as is obvious from Eq. (25). The corresponding experiment²¹ shows an evident decrease of the cross section at $k_a = k_b$. However, these data cannot be directly compared with the predictions of Fig. 1, since another competing channel for the double emission is not considered here, namely, that of single photoelectron emission followed by electron-electron inelastic collision. In contrast to gaseous targets, like in atomic physics, this channel is expected to be quite strong for metallic samples due to the much higher density of the active electrons.

In the second example we consider the case of Fig. 1 for grazing photon incidence, i.e., for nearly p polarization. As is evident from Eq. (25), the factor $\hat{\mathbf{e}} \cdot (\mathbf{k}_a + \mathbf{k}_b)$ implies a maximum intensity when the center-of-mass momentum is parallel to the polarization vector, which is clearly confirmed by Fig. 2.

For the two-electron band, we define a Fermi energy $E_F = 2\epsilon_F$. In Fig. 1, the double emission occurred from states just below E_F . For double emission from the bottom of the two-electron band, we observe a squeezing of the distribution toward equal energy sharing, as seen in Fig. 3. This effect has also been experimentally observed. Till now I have no profound explanation for this trend that also showed up in equivalent calculations for Al and Ni targets.

VI. CONCLUSION

In this work a theory has been presented for the treatment of one-photon–two-electron excitation from solids and surfaces. It has been argued that this process is a footprint of electron-electron coupling in the final and/or initial state.

From the mathematical analysis, it has been inferred that the pairs' spectra are subject to certain selection rules that lead to vanishing emission intensity when the vector momentum of the pair is perpendicular to the polarization vector. In addition, it has been shown that the excited pair undergoes a diffraction from the lattice when their center-of-mass vector momentum changes by multiples of a reciprocal vector. Starting from single-particle jellium states for the delocalized conduction electrons, the optical transition amplitude has been derived analytically. Numerical examples for clean Cu crystal have been presented.

ACKNOWLEDGMENTS

I am indebted to Professor J. Kirschner, Ralf Herrmann, and Serguei Samarin for many enlightening discussions and suggestions.

APPENDIX: ANALYTICAL EVALUATION OF DIPOLE-TRANSITION AMPLITUDE

In this appendix I derive an expression for the transition amplitude M_{fi} [Eq. (6)] using the approximate initial and final states, given by Eqs. (17) and (21), respectively. For the electron-electron interaction V_{ee} I assume a screened Coulomb potential with a screening constant λ , i.e.,

$$V_{ee} = \frac{\exp(-\lambda|\mathbf{r}_a - \mathbf{r}_b|)}{|\mathbf{r}_a - \mathbf{r}_b|}. \quad (\text{A1})$$

Upon inserting a complete set of plane waves $|\mathbf{q}_1, \mathbf{q}_2\rangle$, M_{fi} can be written in the form

$$M_{fi}^{mn} = \frac{1}{\sqrt{2}} \int \int d^3\mathbf{q}_1 d^3\mathbf{q}_2 \langle \mathbf{k}_a, \mathbf{k}_b | V_{ee} G_{ee}^+ [\hat{\mathbf{e}} \cdot (\mathbf{p}_a + \mathbf{p}_b)] | \mathbf{q}_1, \mathbf{q}_2 \rangle \tilde{\phi}_{\epsilon_m, \mathbf{k}'_m}(\mathbf{q}_1) \tilde{\phi}_{\epsilon_n, \mathbf{k}'_n}(\mathbf{q}_2); m \neq n \in \{a, b\}. \quad (\text{A5})$$

The two-body Green operator G_{ee}^+ satisfies an iterative integral equation similar to Eq. (20) with V being replaced by V_{ee} . That is, in a perturbative sense, the interelectronic interaction is taken into account to infinite order. Unfortunately, it has not yet been possible to evaluate Eq. (A5) with the full G_{ee}^+ . Thus we replace G_{ee}^+ by the free Green operator G_0^+ , and V_{ee} is treated to first order [this approximation is less severe than in atomic and molecular reactions since the potential (A1) is screened]. The expressions (A5) are obtained from the integral

$$\begin{aligned} J &= \int \int d^3\mathbf{q}_1 d^3\mathbf{q}_2 \langle \mathbf{k}_a, \mathbf{k}_b | V_{ee} G_0^+ (\hat{\mathbf{e}} \cdot \mathbf{p}_a) | \mathbf{q}_1, \mathbf{q}_2 \rangle \tilde{\phi}_{\epsilon_a, \mathbf{k}'_a}(\mathbf{q}_1) \tilde{\phi}_{\epsilon_b, \mathbf{k}'_b}(\mathbf{q}_2) \\ &= \lim_{\eta \rightarrow 0^+} \int \int d^3\mathbf{q}_1 d^3\mathbf{q}_2 (\hat{\mathbf{e}} \cdot \mathbf{q}_1) \langle \mathbf{k}_a, \mathbf{k}_b | V_{ee} | \mathbf{q}_1, \mathbf{q}_2 \rangle \frac{\tilde{\phi}_{\epsilon_a, \mathbf{k}'_a}(\mathbf{q}_1) \tilde{\phi}_{\epsilon_b, \mathbf{k}'_b}(\mathbf{q}_2)}{k_a^2 + k_b^2 - q_1^2 - q_2^2 - i\eta} \\ &= \frac{\lim_{\eta \rightarrow 0^+}}{2\pi^2} \int \int d^3\mathbf{q}_1 d^3\mathbf{q}_2 (\hat{\mathbf{e}} \cdot \mathbf{q}_1) [(\mathbf{q}_2 - \mathbf{k}_b)^2 + \lambda^2]^{-1} (k_a^2 + k_b^2 - q_1^2 - q_2^2 - i\eta)^{-1} \\ &\quad \times \tilde{\phi}_{\epsilon_a, \mathbf{k}'_a}(\mathbf{q}_1) \tilde{\phi}_{\epsilon_b, \mathbf{k}'_b}(\mathbf{q}_2) \delta^{(3)}(\mathbf{q}_1 + \mathbf{q}_2 - \mathbf{k}_a - \mathbf{k}_b). \end{aligned} \quad (\text{A6})$$

Writing $\hat{\mathbf{e}} \cdot \mathbf{q}_1 = -i \lim_{\beta \rightarrow 0} \partial_\beta \exp(i\beta \hat{\mathbf{e}} \cdot \mathbf{q}_1)$, and using the δ function to perform one of the integrations, Eq. (A6) reduces to

$$J = \frac{\lim_{\eta, \beta \rightarrow 0^+}}{i2\pi^2} \partial_\beta \int d^3\mathbf{q} [(\mathbf{q}_2 - \mathbf{k}_b)^2 + \lambda^2]^{-1} [-2q^2 - 2\mathbf{k}_a \cdot \mathbf{k}_b + 2\mathbf{q} \cdot (\mathbf{k}_a + \mathbf{k}_b) - i\eta]^{-1} \tilde{\phi}_{\epsilon_a, \mathbf{k}'_a}(\mathbf{q}) \tilde{\phi}_{\epsilon_b, \mathbf{k}'_b}(\Lambda) \exp(i\beta \hat{\mathbf{e}} \cdot \mathbf{q}_1), \quad (\text{A7})$$

where $\Lambda := \mathbf{k}_a + \mathbf{k}_b - \mathbf{q}$. Making use of Eq. (A3), and upon some elementary algebraic manipulation, Eq. (A7) is transformed to the one-dimensional integral on the real axis:

$$\begin{aligned} M_{fi}(\mathbf{k}_a, \mathbf{k}_b) &= \int \int d^3\mathbf{q}_1 d^3\mathbf{q}_2 \langle \mathbf{k}_a, \mathbf{k}_b | (1 + V_{ee} G_{ee}^+) \\ &\quad \times [\hat{\mathbf{e}} \cdot (\mathbf{p}_a + \mathbf{p}_b)] | \mathbf{q}_1, \mathbf{q}_2 \rangle \langle \mathbf{q}_1, \mathbf{q}_2 | \psi_{\epsilon_i} \rangle \\ &= \hat{\mathbf{e}} \cdot (\mathbf{k}_a + \mathbf{k}_b) \tilde{\psi}(\mathbf{k}_a, \mathbf{k}_b) + M_{fi}^{ab} + M_{fi}^{ba}, \end{aligned} \quad (\text{A2})$$

where the double Fourier transform $\tilde{\psi}(\mathbf{k}_a, \mathbf{k}_b)$ is easily constructed from the Fourier transform of the single-particle jellium wave functions $\tilde{\phi}(\mathbf{k}_j), j = a, b$,

$$\tilde{\phi}_{\mathbf{k}'_j}(\mathbf{k}_j) = i \sqrt{\frac{2\pi}{V}} \delta^{(2)}(\mathbf{k}'_{j\parallel} - \mathbf{k}_{j\parallel}) L_{\mathbf{k}'_j}(\mathbf{k}_j), \quad (\text{A3})$$

where

$$L_{\mathbf{k}'_j}(\mathbf{k}_j) = \left(\frac{1}{\mathbf{k}_{j,z} - \mathbf{k}'_{j,z} + i\delta} + \frac{R_j}{\mathbf{k}_{j,z} + \mathbf{k}'_{j,z} + i\delta} - \frac{T_j}{\mathbf{k}_{j,z} - i\gamma_j} \right). \quad (\text{A4})$$

The infinitesimal real variable $\delta > 0$ has been introduced to account for the finite extension of the surface in the direction $z < 0$, and can be set to zero (infinite extension) in the final result. Formally, the first term in expression (A2) should vanish, since initial and final states are combinations of independent single-particle states. In fact, numerical investigations have shown that magnitude of this term is negligibly small with respect to the terms $|M_{fi}^{mn}|$; $m, n = a, b$.

The terms $|M_{fi}^{mn}|$; $m \neq n \in \{a, b\}$ are defined as

$$J = \frac{\lim_{\eta, \beta, \delta \rightarrow 0^+}}{i2\pi V} \partial_\beta [\exp(i\beta \hat{\mathbf{e}}_{\parallel} \cdot \mathbf{k}'_{a,\parallel}) \delta^{(2)}(\mathbf{k}'_{a,\parallel} + \mathbf{k}'_{b,\parallel} - \mathbf{k}_{a,\parallel} + \mathbf{k}_{b,\parallel}) I]. \quad (\text{A8})$$

The integral I can be written as the sum of nine one-dimensional integrals

$$I(\epsilon_a, \mathbf{k}'_a, \epsilon_b, \mathbf{k}'_b; \mathbf{k}_a, \mathbf{k}_b) := \sum_{j=1}^9 \int_{-\infty}^{\infty} dq_z II_j(q_z, \epsilon_a, \mathbf{k}'_a, \epsilon_b, \mathbf{k}'_b; \mathbf{k}_a, \mathbf{k}_b), \quad (\text{A9})$$

where

$$II_1 = \exp(i\beta \hat{\mathbf{e}}_z q_z) A^{-1}(q_z) B^{-1}(q_z) (q_z - k'_{a,z} + i\delta)^{-1} (q_z - k_{a,z} - k_{b,z} + k'_{b,z} - i\delta)^{-1}, \quad (\text{A10})$$

$$II_2 = R_b \exp(i\beta \hat{\mathbf{e}}_z q_z) A^{-1}(q_z) B^{-1}(q_z) (q_z - k'_{a,z} + i\delta)^{-1} (q_z - k_{a,z} - k_{b,z} - k'_{b,z} - i\delta)^{-1}, \quad (\text{A11})$$

$$II_3 = -T_b \exp(i\beta \hat{\mathbf{e}}_z q_z) A^{-1}(q_z) B^{-1}(q_z) (q_z - k'_{a,z} + i\delta)^{-1} (q_z - k_{a,z} - k_{b,z} + i\gamma_b)^{-1}, \quad (\text{A12})$$

$$II_4 = R_a \exp(i\beta \hat{\mathbf{e}}_z q_z) A^{-1}(q_z) B^{-1}(q_z) (q_z + k'_{a,z} + i\delta)^{-1} (q_z - k_{a,z} - k_{b,z} + k'_{b,z} - i\delta)^{-1}, \quad (\text{A13})$$

$$II_5 = R_a R_b \exp(i\beta \hat{\mathbf{e}}_z q_z) A^{-1}(q_z) B^{-1}(q_z) (q_z + k'_{a,z} + i\delta)^{-1} (q_z - k_{a,z} - k_{b,z} - k'_{b,z} - i\delta)^{-1}, \quad (\text{A14})$$

$$II_6 = -R_a T_b \exp(i\beta \hat{\mathbf{e}}_z q_z) A^{-1}(q_z) B^{-1}(q_z) (q_z + k'_{a,z} + i\delta)^{-1} (q_z - k_{a,z} - k_{b,z} + i\gamma_b)^{-1}, \quad (\text{A15})$$

$$II_7 = -T_a \exp(i\beta \hat{\mathbf{e}}_z q_z) A^{-1}(q_z) B^{-1}(q_z) (q_z - i\gamma_a)^{-1} (q_z - k_{a,z} - k_{b,z} + k'_{b,z} - i\delta)^{-1}, \quad (\text{A16})$$

$$II_8 = -T_a R_b \exp(i\beta \hat{\mathbf{e}}_z q_z) A^{-1}(q_z) B^{-1}(q_z) (q_z - i\gamma_a)^{-1} (q_z - k_{a,z} - k_{b,z} - k'_{b,z} - i\delta)^{-1}, \quad (\text{A17})$$

$$II_9 = T_a T_b \exp(i\beta \hat{\mathbf{e}}_z q_z) A^{-1}(q_z) B^{-1}(q_z) (q_z - i\gamma_a)^{-1} (q_z - k_{a,z} - k_{b,z} + i\gamma_b)^{-1}. \quad (\text{A18})$$

The functions $A(q_z)$ and $B(q_z)$ possess the forms

$$A(q_z) = (k_{a,z} - q_z)^2 + (\mathbf{k}_{a,\parallel} - \mathbf{k}'_{a,\parallel})^2 + \lambda^2, \quad (\text{A19})$$

$$B(q_z) = q_z^2 - q_z(k_{a,z} + k_{b,z}) + \mathbf{k}_a \cdot \mathbf{k}_b + \mathbf{k}'_{a,\parallel}{}^2 - \mathbf{k}'_{a,\parallel} \cdot (\mathbf{k}_{a,\parallel} + \mathbf{k}_{b,\parallel}) + i\eta/2. \quad (\text{A20})$$

To evaluate the integrals $II_j, j=1, \dots, 9$ we convert q_z to a complex variable, and consider the improper contour integrals

$$I = \sum_{j=1}^9 \lim_{\rho \rightarrow \infty} \oint_{\partial G_\rho} dq_z II_j(q_z). \quad (\text{A21})$$

The compact domain G is chosen as the upper half of the complex plane, i.e., $G = \{q_z | \Im(q_z) > 0, |q_z| < \rho\}$. From the preceding analytical expressions of II_j it is readily deduced

that only isolated singularities of II_j occur in G , i.e., $II_j(q_z)$ are meromorphic in G . Integral (A9) can thus be evaluated via calculus of residues.

The poles of $II_1(q_z)$ are deduced to

$$z_{11}^\pm = k_{a,z} \pm i\sqrt{(\mathbf{k}_{a,\parallel} - \mathbf{k}'_{a,\parallel})^2 + \lambda^2}, \quad (\text{A22})$$

$$z_{21}^\pm = -b/2 \pm \sqrt{\rho_z} (\cos \varphi/2 + i \sin \varphi/2), \quad (\text{A23})$$

$$z_{41} = k_{a,z} + k_{b,z} - \mathbf{k}'_{b,z} + i\delta, \quad (\text{A24})$$

where $b := k_{a,z} + k_{b,z}, \rho_z := \sqrt{(b^2 - 4d)^2 + \eta^2/4}, d := \mathbf{k}_a \cdot \mathbf{k}_b + k'_{a,\parallel}{}^2 - \mathbf{k}'_{a,\parallel} \cdot (\mathbf{k}_{a,\parallel} + \mathbf{k}_{b,\parallel})$, and $\sin \varphi = -\eta/(2\rho_z) < 0$. In G the function II_1 possesses the poles z_{11}^+, z_{21}^- , and z_{41} . The poles of II_2 in G are $z_{12}^+ \equiv z_{11}^-, z_{22}^- \equiv z_{21}^-$, and z_{42} , where $z_{42} = k_{a,z} + k_{b,z} + \mathbf{k}'_{b,z} + i\delta$. The singularities of II_3 in G are $z_{13}^+ \equiv z_{11}^-$ and $z_{23}^- \equiv z_{21}^-$. The poles of II_4 in G are deduced to $z_{14}^+ \equiv z_{11}^-, z_{24}^- \equiv z_{21}^-$, and $z_{44} \equiv z_{41}$. II_5 possesses in G poles

$z_{15}^+ \equiv z_{11}^-$, $z_{25}^- \equiv z_{21}^-$, and $z_{45} \equiv z_{42}$. II_6 , in G , has the poles $z_{16}^+ \equiv z_{11}^-$, and $z_{26}^- \equiv z_{21}^-$. The singularities of II_7 in G are $z_{17}^+ \equiv z_{11}^-$, $z_{27}^- \equiv z_{21}^-$, $z_{37} = i\gamma_a$, and z_{47} , where $z_{47} = z_{41}$. The singularities of II_8 that occur in G are $z_{18}^+ \equiv z_{11}^-$, $z_{28}^- \equiv z_{21}^-$, $z_{38} \equiv z_{37}$, and $z_{48} \equiv z_{42}$. Finally, the poles of II_9 in G are $z_{19}^+ \equiv z_{11}^-$, $z_{29}^- \equiv z_{21}^-$, and $z_{39} \equiv z_{38}$.

The integral I can then be written in closed form

$$I = 2\pi i \sum_{j=1}^9 \sum_{\nu} \text{Res}_{\nu j} II_j(q_z). \quad (\text{A25})$$

Upon substitution of Eq. (A25) into Eq. (A8), and performing the derivatives and the limits, an analytical, however complicated, expression for the dipole-transition amplitude (A5) is obtained (within the approximation $G_{ee}^+ \approx G_0^+$).

-
- ¹ *Angle-Resolved Photoemission: Theory and Current Application*, edited by S. D. Kevan, Studies in Surface Science and Catalysis (Elsevier, Amsterdam, 1992).
- ² S. Hüfner, *Photoelectron Spectroscopy*, in Springer Series in Solid-State Science Vol. 82 (Springer-Verlag, Berlin, 1995).
- ³ J. Braun, Rep. Prog. Phys. **59**, 1267 (1996).
- ⁴ P. Hohenberg and W. Kohn, Phys. Rev. B **136**, 864 (1964).
- ⁵ R. M. Dreizler and E. K. U. Gross, *Density Functional Theory* (Springer-Verlag, Berlin, 1990).
- ⁶ V. Schmidt, *Electron Spectrometry of Atoms using Synchrotron Radiation*, Cambridge Monographs on Atomic, Molecular and Chemical Physics (Cambridge University Press, Cambridge, 1997).
- ⁷ O. Schwartzkopf, B. Krässig, J. Elmiger, and V. Schmidt, Phys. Rev. Lett. **70**, 3008 (1993).
- ⁸ P. Lablanquie, J. Mazeau, L. Andric, P. Selles, and A. Huetz, Phys. Rev. Lett. **74**, 2192 (1995).
- ⁹ A. Huetz, L. Andric, A. Jean, P. Lablanquie, P. Selles, and J. Mazeau, in *The Physics of Electronic and Atomic Collisions*, Proceedings of XIX ICPEAC, Whistler, edited by L. Dube' *et al.*, AIP Conf. Proc. No. 360 (AIP, New York, 1995).
- ¹⁰ G. Dawber, L. Avaldi, A. G. McConkey, H. Rojas, M. A. McDonald, G. C. King, F. Heiser, R. Hentgens, O. Gessner, and A. Rüdél, J. Phys. B **28**, L271 (1995).
- ¹¹ J. Vieffhaus, L. Avaldi, F. Heiser, R. Hentgens, O. Gessner, A. Rüdél, M. Wiedenhöft, K. Wieliczek, and U. Becker, J. Phys. B **29**, L729 (1996).
- ¹² R. Dörner, J. Feagin, C. L. Cocke, H. Bräuning, O. Jagutzki, M. Jung, E. P. Kanter, H. Khemliche, S. Kravis, V. Mergel, M. H. Prior, H. Schmidt-Böcking, L. Spielberger, J. Ullrich, M. Unverzagt, and T. Vogt, Phys. Rev. Lett. **77**, 1024 (1996).
- ¹³ F. Maulbetsch and J. S. Briggs, J. Phys. B **28**, 551 (1995).
- ¹⁴ M. Pont and R. Shakeshaft, Phys. Rev. A **51**, R2676 (1995).
- ¹⁵ A. K. Kazansky and V. N. Ostrovsky, J. Phys. B **26**, 2231 (1993).
- ¹⁶ A. W. Malcherek, F. Maulbetsch, and J. S. Briggs, J. Phys. B **29**, 4127 (1996).
- ¹⁷ J. Berakdar and H. Klar, Phys. Rev. Lett. **69**, 1175 (1992); J. Phys. B **26**, 4219 (1993).
- ¹⁸ J. Berakdar, H. Klar, A. Huetz, and P. Selles, J. Phys. B **26**, 1463 (1993).
- ¹⁹ J. Vieffhaus, L. Avaldi, G. Snell, M. Wiedenhöft, R. Hentgens, A. Rüdél, F. Schäfers, D. Menke, U. Heinzmann, A. Engelns, J. Berakdar, H. Klar, and U. Becker, Phys. Rev. Lett. **77**, 3975 (1996).
- ²⁰ V. Mergel, M. Achler, R. Dörner, KH. Khayyat, T. Kambara, Y. Awaya, V. Zoran, B. Nyström, L. Spielberger, J. H. McGuire, J. Feagin, J. Berakdar, Y. Azuma, and H. Schmidt-Böcking, Phys. Rev. Lett. **80**, 5301 (1998).
- ²¹ R. Herrmann, S. N. Samarin, H. Schwabe, and J. Kirschner, Phys. Rev. Lett. (to be published).
- ²² P. J. Feibelman, Surf. Sci. **46**, 558 (1974).
- ²³ H. J. Levinson, E. W. Plummer, and P. J. Feibelman, Phys. Rev. Lett. **43**, 942 (1979).
- ²⁴ J. B. Pendry, in *Photoemission and the Electronic Properties of Surfaces*, edited by B. Feuerbacher, B. Fitton, and R. Willis (Wiley, New York, 1978), p. 87.
- ²⁵ L. D. Landau and E. M. Lifschitz, *Lehrbuch der theoretischen Physik Vol. III: Quantenmechanik* (Akademie Verlag, Berlin, 1979).
- ²⁶ J. P. Taylor, *Scattering Theory* (Wiley, New York, 1972).
- ²⁷ W. Nolting, *Viel-Teilchen-Theorie*, 2nd ed. (Verlag Zimmermann-Neufang, Ulmen, 1992).
- ²⁸ G. D. Mahan, *Many-Particle Physics*, 2nd ed. (Plenum, New York, 1993).
- ²⁹ C. Kittel, *Introduction to Solid State Physics*, 3rd ed. (Wiley, New York, 1966).
- ³⁰ J. B. Pendry, *Low Energy Electron Diffraction* (Academic, London, 1974).